# Chapter 5

# Fabrication of a Schottky based ISFET immobilized with enzyme CYP450

## 5.1 Introduction

Fabrication of ISFET is almost similar to MOSFET; hence the existing CMOS technology and process are being employed to fabricate ISFET. Conventional ISFET has number of fabrication steps which makes the process complex, time-consuming and expensive. More the number of lithography steps, higher is the process cost involved. Therefore, a new fabrication technique was developed to replace doped silicon source/drain(S/D) region with metal S/D. Thus, Schottky barrier (SB) MOSFET came into being. In this work, this idea of Schottky barrier MOSFET has been extended to fabricate ISFET. Further, this Schottky ISFET is immobilized with cytochrome P450 and made into an ENFET and also is characterized into mercury MOSFET.

The idea of completely replacing doped Source/Drain (S/D) regions with metal was proposed by Nishi in 1966 when he submitted a Japanese patent on the idea [1]. It was issued later in 1970. Lepselter and Sze in 1968, published the first paper describing a PMOS bulk device employing PtSi for the source/drain (S/D) regions [2]. In the eighties, a variety of SB-MOS device structures were studied such as the first SB-NMOS device by Mochizuki and Wise [3], devices employing interfacial doping layers between the metal S/D and the channel[4], and asymmetric devices in which the source is metal and drain is doped silicon[5]. Sugino et al.[6] and Swirhun et al.[7] indicated that the SB MOS can eliminate parasitic bipolar action. Tucker et al.[8], and Synder et al.[9] realized the advantages for device scaling of SB- MOS technology and had indicated in their works. The state of the art of SB-MOS technology has progressed significantly in the last decade.

When certain metals are deposited directly on semiconductor it forms Schottky contact if the barrier height is large ( $\phi_B > kT$ ) [10]. Since the substrate considered in this work is p type, the Schottky barrier height ($\phi_{Bp}$) can be expressed as the difference between the valence band edge and the Fermi energy in the metal [11],

$$\phi_{Bp} = \frac{E_g}{q} + \chi - \phi_m \tag{5.1}$$

Here $E_g$ is the band gap of silicon semiconductor which is 1.12eV, $q$ is the electronic charge, $\chi$ is the electron affinity which is 4.01 V for silicon, $\phi_m$ is the work function of metal (here silver) which is 4.26V. The barrier height obtained is 0.91V which is greater than the value of $kT$ thus indicating the formation of a Schottky contact [11].

**5.2 Principle of operation**

The principle can be understood by drawing an analogy with an SB MOS device. For an SB MOS device, the S/D- to substrate junction is fundamentally different than that of a conventional MOSFET device with doped source and drain regions [12, 13]. At the S/D junction, doped conventional MOSFET forms a p-n diode junction. Conversely, metal S/D SB MOS devices form an abrupt SB junction having an SB height. Instead of the continuous energy band profiles present in conventional MOSFETs, the valence and conduction bands in a SB-MOSFET contain abrupt junctions between metallic and semiconducting materials at either end of the channel. Traversing through the length of the MOSFET, the carriers must travel through metal, then semiconductor and then metal again as illustrated in figure 5.1. In the metal source, carriers drift under the influence of the applied field until they reach the source to channel interface. On application of negative bias, the majority carriers accumulate at the semiconductor-gate dielectric interface. Conversely, on the application of positive bias to the p-type Schottky ISFET, the body depletes and eventually with higher positive bias it inverts to form an n-type channel. If the barrier height for hole is large, the inversion mode (electron) barrier height is relatively small [13, 14]. Positive bias, when applied to the gate, leads toward band bending (downwards) in the region below the oxide. This inversion caused by band bending consequently reduces the contact potential built up due to metal/semiconductor contact, leading to flow of electrons between source and drain through the channel [14].

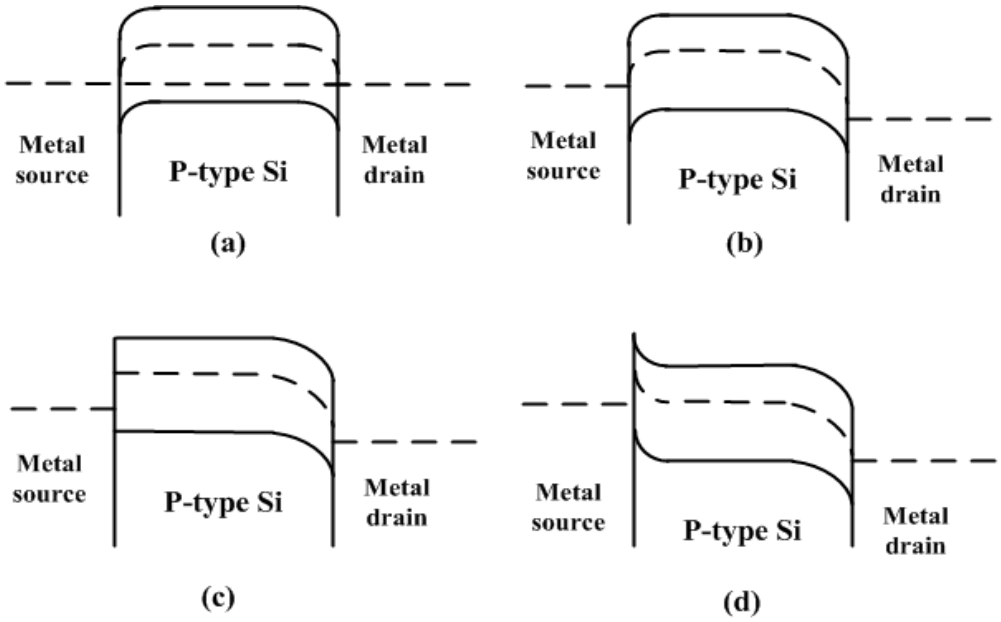


Figure 5. 1: Energy band diagram for a n channel SB MOSFET illustrating four states of operation (a) OFF state; $V_{GS}$= 0, $V_{DS}$= 0 (b) OFF state; $V_{GS}$= 0, $V_{DS}$ > 0 (c) $V_{GS}$< $V_T$, $V_{DS}$ > 0 (d) ON state; $V_{GS}$> $V_T$, $V_{DS}$ > 0 [13]

The SB ISFET explained here too works under the same principle as in SB MOSFET in the semiconductor side. In the case of electrolyte insulator interface ISFET as explained in Chapter 2, follows the two important theory- site binding theory and the formation of electrical double layer. The hydrogen ion present in the electrolyte will react with the active sites of the insulating layer. This will bring about a redistribution of the charges at the interface of the electrolyte insulator thus varying the interfacial potential. This can be well detected by the change in the drain current. Further, when the sensing layer of the ISFET is immobilized with the enzyme, the change in the concentration of the analyte after reacting with the enzyme is well detected by the underlying ISFET device.

The fabrication details and characterization of the ISFET, ISFET based biosensor and the Hg MOSFET are described in the following paragraph.

### 5.3 Fabrication of the ISFET

A 3″ double sided polished p type silicon wafer (100) with a resistivity of about 1-10Ω cm has been used as the substrate for the fabrication of ISFET device. The wafer is boron doped and has a thickness of about 380μm. The several steps which are involved in device fabrication are stated as follows-

*Degreasing*

Degreasing of the wafer was done to remove wax or any oil contamination. The degreasing process involves treating the wafers firstly with acetone at a mild temperature (< 50°C) for 5 minutes, followed by rinsing in De-ionized (DI) water .Further methanol treatment was done at 50°C for 5 minutes and again rinsing in DI water. These steps help to remove any oil contamination. Finally, the wafer was again treated with acetone, as it helps in removal of any traces of methanol if present.

*RCA cleaning processes*

Radio Corporation of America (RCA) is a standard set of wafer cleaning steps which follows the degreasing process. The RCA (SC-1) process involves mixing 4 ml of ammonium hydroxide, 4 ml of hydrogen peroxide and 20 ml of DI water in a beaker with the wafer placed in it. This was followed by rinsing in DI water and immediately placing the wafers in hydrofluoric acid (HF acid) bath for the oxide clean. Wafer was dipped into a solution containing 1 part of HF acid mixed with 30 parts of DI water in a teflon beaker. This etches the native oxide formed at the surface. The wafer was further rinsed in DI water to remove traces of HF and immediately transferred to hot standard clean no 2 (SC 2) solution. This step removes the ionic and heavy metal atomic contaminants. 1 part of hydrogen peroxide, 1 part of Hydrochloric acid mixed in 6 part of DI water was taken in a beaker (Acid added to water and not vice versa). The wafer was submerged into this bath for 10 minutes. The wafer was rinsed in DI water immediately after this treatment and dried with a nitrogen gun.

*Piranha cleaning (optional)*

After the oxide is deposited if any cleaning is required than piranha cleaning can be carried out. It involves dipping the wafer into a mixture of sulphuric acid and hydrogen peroxide in 5:1 ratio at a temperature of 80°C for 5 minutes, followed by rinsing in DI water.

*Thermal oxidation*

After the wafers are degreased and RCA treated, silicon dioxide layer was deposited by thermal oxidation at a temperature of 1050°C with a gas flow of 2slpm (standard liquid per minute) of oxygen for a duration of 30 minutes /1 hour/ 30 minutes to follow the standard dry, wet and again dry technique of deposition. Oxide thickness of 480nm is achieved in this process.

*Lithography*

This was followed by the lithography process for transferring patterns on the wafer from the mask. Lithography process involves steps such as coating the wafer with photoresist. Here positive photo resist (Microchem S1818) was used, where the wafer was spun on a turntable at a high speed for evenly spreading the resist all over the wafer. The photoresist coated wafer was baked on a hot plate for 5 seconds (hard contact) and then cooled. The wafer becomes ready for lithography after this step. Contact lithography was used for exposing the photoresist through the pattern mask to a UV light of 420 nm. The photoresist was developed and the developer (Microchem CD26) was used for the purpose. After developing the pattern, post-baking was carried out. This usually hardens the final resist image so that it can withstand the harsh environment of implantation or etching. Therefore the first lithography process was done using the first mask (Figure 5.2 a inset) which outlines the area of 22×7 $mm^2$ comprising of the active area and the protective region. The protective region was given, so as to prevent the metal from coming into direct contact with the active area. The masked region was well protected by the photoresist and from the unmasked region; silicon dioxide was completely etched out using buffer oxide etchant. Once the etching was over the photoresist was removed using acetone. Second lithography process was carried out to etch out the active area of dimension 5×5 $mm^2$ by using a

second mask (Figure 5.2. b inset). This second lithography process had similar steps as that of the first. Here the etching was done partially and the thickness of the insulating layer at the active region was found to be about 120nm (measured by Metricon 2010M prism coupler). A hard mask was used as the third mask for the metal deposition. Here the first mask was used again as the hard mask. This mask is a transparent sheet with the imprints of first mask and opening are present at the regions where the metal has to be deposited. This technique of using hard mask avoids the necessity of another level of lithography and makes it cost effective. The hard mask was carefully attached to the wafer using Kapton tape (Polymide film which can sustain high temperature). The wafer with the attached mask was introduced in the thermal evaporator to deposit the metal.

*Metallization and final packaging*

A 200 nm thick silver layer was deposited for metal contact on the exposed region to form a Schottky contact at 60-70A current for a duration of 30seconds.The wafer after the metal deposition was mounted on a PCB board with adhesives. The connections for the source, gate and drain terminals was obtained by soldering male connectors at the PCB board. These connectors further were bonded to the metal layers using silver paste. Since the measurand has to be in direct contact of the sensing layer, hence a glass chamber has to be formed over the sensing layer of the ISFET so that it can hold the measurand. This chamber was constructed using cover slip. For passivation and sealing purpose silicone was used. Prior to induction, the silicone was tested which showed neutral effects to pH changes even when exposed for longer duration of time. The masks were designed using *Clewin software* version 4. The schematics of the process flow showing the fabrication process has been depicted in figure 5.2 and the actual device has been shown in figure. 5.2.e (inset).

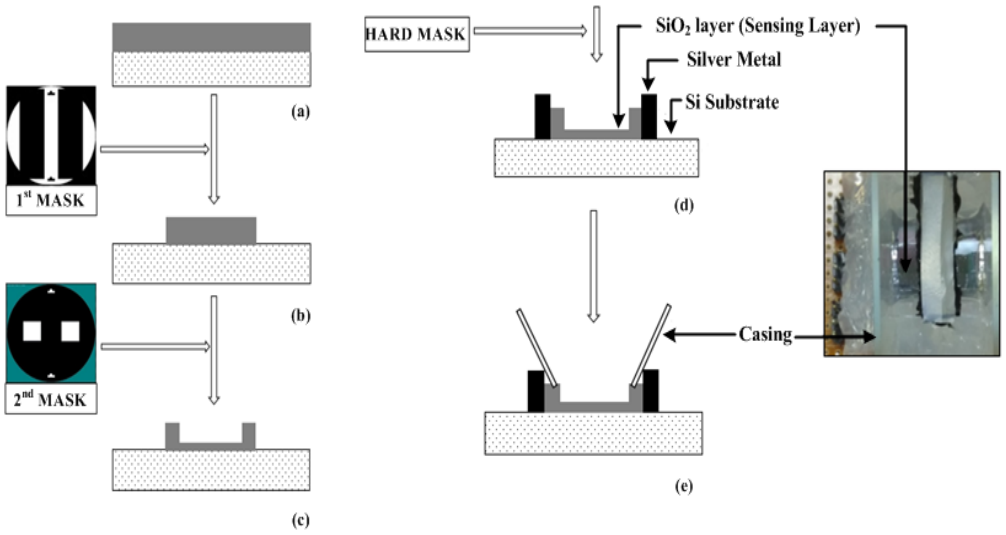


Figure 5.2. Figure showing the schematics of the process flow of the fabrication process (a) Thermal oxidation on clean silicon p type wafer (b) First lithography using the first mask (inset) to pattern the region for depositing metal at later stage(c) Second lithography using second mask (inset) defining the active area (d) Metal deposition using the hard mask (e) Casing done using cover slip for safe loading of electrolyte on the active area, (inset: The actual picture of the device)

### 5.3.1 ISFET made into an ENFET

The fabricated ISFET device was further immobilized with the enzyme Cytochrome P450 to form an Enzyme FET termed here as CYPFET. This enzyme has affinity towards various hydrocarbon species like simple hydrocarbons such as alkanes, alkenes, alkynes and also poly aromatic hydrocarbons [15].

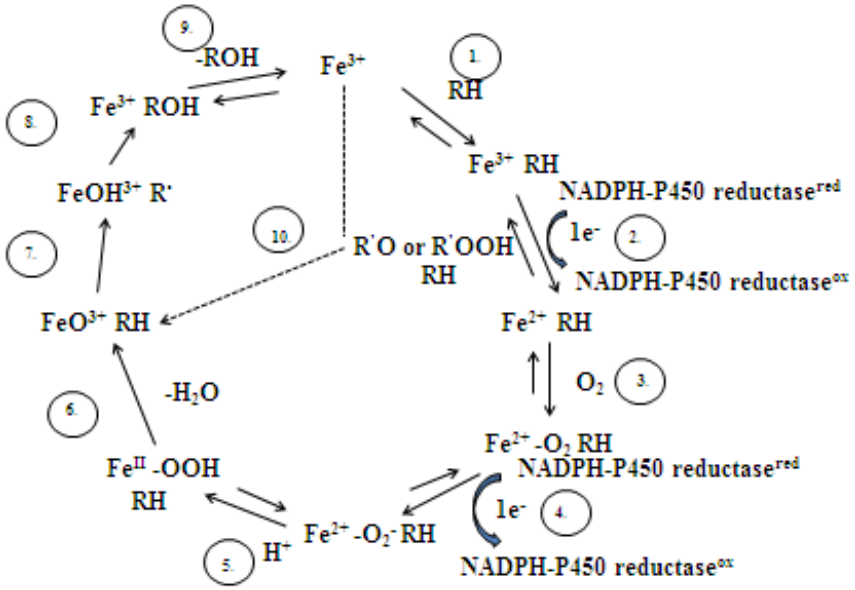


Figure 5.3. Figure showing generalized catalytic cycle for P450.Only the heme iron of P450 is shown to represent the active site of the P450. The abbreviations are as follows: Fe, iron atom in P450 heme; RH, substrate; ROH, product; ox and red, the reduced and (1-electron) oxidized states of P450 reductase involved in electron transfers (under "Catalysis by P450s"). The figure was adapted from [16]

The basic catalytic cycle for cytochrome P450s involves several steps, as outlined in figure 5.3. The cycle starts with binding of the substrate to oxidized P450 (step 1). Following this binding, the NADPH-P540 reductase provides the first electron to the P450, to reduce the P450 heme to the ferrous state (step 2). Molecular oxygen then binds to the ferrous P450 followed by transfer of a second electron and activation of oxygen (steps 3 and 4). The addition of a hydrogen ion (step 5) is followed by O–O bond cleavage and $H_2O$ is released (step 6). An electron-deficient $FeO_3$ formal complex is left behind. This complex then abstracts a hydrogen atom or an electron from the substrate to produce a substrate radical (step 7), and the "second" atom of oxygen is transferred to the incipient substrate radical (step 8). Finally, with the heme iron returning to the ferric state the product is released (step 9) [17]. The generalized reaction can be explained in a simplified manner such that two protons are consumed in every cycle of the reaction. This will make a local shift in the pH in the enzyme layer. This change in pH will be detected by the underlying ISFET. The basic reaction can be stated as-

$$RH + O_2 + 2H^+(\text{from } NADPH) \xrightarrow{CYP450} ROH + H_2O \qquad (5.2)$$

In the stated reaction RH is a substrate with a hydroxylatable site. In each reaction cycle, one molecular oxygen is inserted by the enzyme cytochrome P450 monooxygenase making it ROH [18]. In case of ENFET, in addition to the site binding theory and electrical double layer theory an electrolyte biological insulator semiconductor system has to be considered for ENFET modeling.

The same ISFET device is used as ENFET hence in the process flow another step has been included as depicted in figure.5.4.

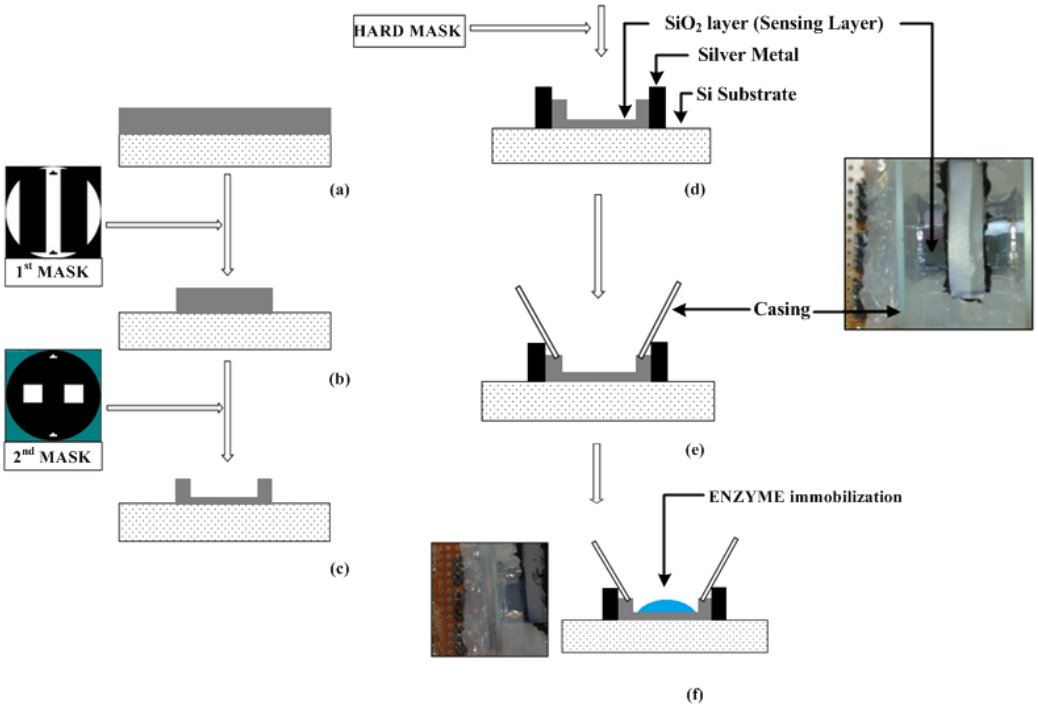


Figure 5.4. Schematic for the process flow of the ENFET fabrication. From (a) to (e) it follows the same step as described in figure 5.2. (f) device after immobilization(inset picture of the device after immobilization)

The biologically sensitive element used as biomimetic component of the device was derived from spheroplasts of bacterial strain *Bacillus stratosphericus sp.* as a "partially purified cytochrome P450 enzyme preparation" supplied by

Applied Biochemistry Laboratory, Department of Molecular Biology and Biotechnology, Tezpur University (Sarma and Medhi, unpublished work).

The specific content of enzyme cytochrome P450 present in the spheroplasts prepared was calculated by observing the CO-Fe (II) versus Fe (II) difference spectra [19] using the following formula

$$CYP\ content = [A_{(COAbs450-COAbs490)} - B_{(Abs450-Abs490)}]/91 \quad (5.3)$$

Where *A* is the absorbance spectra after passing through CO, *B* is the absorbance spectra from the baseline spectrum. 91 is the extinction coefficient. (91 $mM^{-1}cm^{-1}$).

**5.3.1.1 Partial purification of the enzyme**

The enzyme to be immobilized has to be purified prior to its use in the ENFET device. The purification process carried has been obtained from literature [20, 21] but modifications were done as per requirement. After an ultracentrifugation processes the sample was purified using gel filtration chromatography (Seralose CL-6B column) followed by anion exchange chromatography (DEAE cellulose column). Further the eluted fractions were tested for CYP content using CO difference spectra [19] after every step of the purification process and finally the fraction showing maximum CYP content was used for the immobilisation process. (Sarma and Medhi, unpublished work).

*Analyte for reaction:*

The analyte which was used for the reaction for the ENFET device was n-hexadecane (purchased from Merck). It is a long chain alkane hydrocarbon with a chemical formula of $C_{16}H_{34}$.

**5. 3.1.2 Enzyme immobilization**

In a vortex, the purified fraction of cytochrome P450 enzyme in 50 mM Tris HCl buffer was mixed with equal volume of agarose (5 % w/v) in 50 mM Tris HCl (pH 7.2). 40 µl from this mixture was laid over the silicon dioxide surface of the fabricated ISFET device using a micropipette, further allowing it to solidify for about 10 minutes [22]. This was done in due collaboration with Applied Biochemistry Laboratory, Department of Molecular Biology and Biotechnology, Tezpur University.

### 5. 3.2 Mercury (Hg) MOSFET

The fabricated ISFET has been also characterised in a form of MOSFET by introducing liquid metal mercury (Hg) as gate over layer. Researches have been carried out to use liquid metal for metallization as other techniques such as vacuum evaporation or electron beam source have the disadvantage of being influenced by crystallographic and chemical nature of the surface of the interfaces and its localised defects [23, 24]. Moreover, using these techniques involves modification of the surface and sometimes it becomes worse for reactive silicon substrate. Conversely, these disadvantages are not witnessed in case of liquid metal. Also, removal of the liquid metal can be done with ease as the surface tension of Hg is high [25]. Therefore, the Hg MOSFET can be easily transformed back into the original fabricated ISFET without any additional etching process. Also, no side effects were observed such as lowering the sensitivity of the fabricated ISFET has been observed at the sensing surface on which the liquid metal was deposited.

Conversion of the ISFET into Hg MOSFET is depicted in figure 5.5.

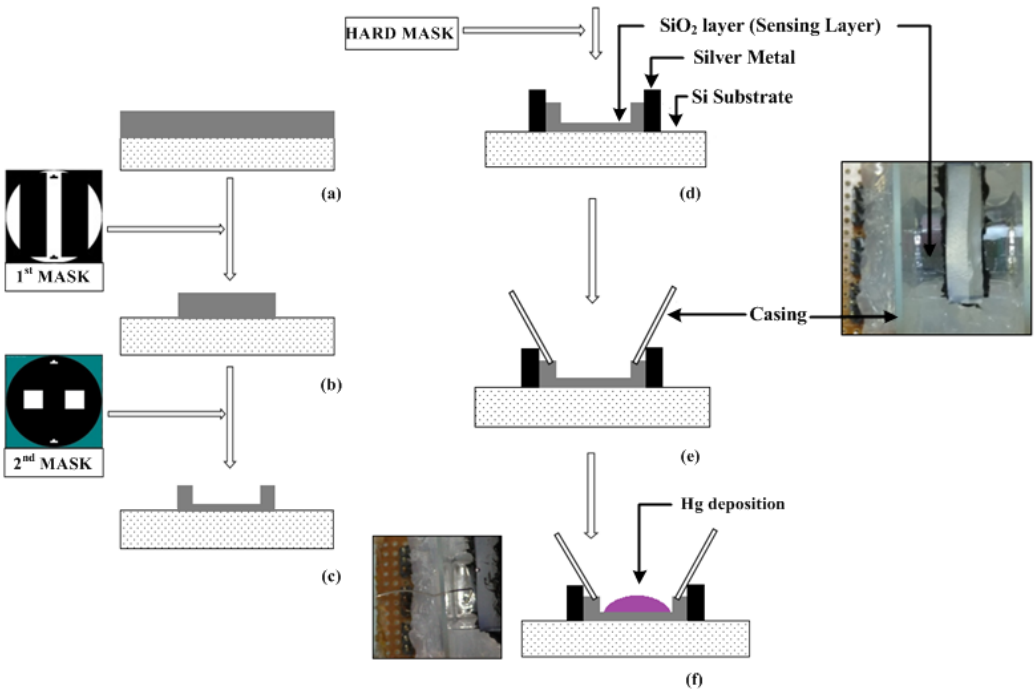


Figure 5.5. Schematic of the process flow of the Hg MOSFET fabrication. From (a) to (e) it follows the same step as described in figure (Figure.5.2). (f) device after mercury is poured on the sensing layer and reference electrode immerse into mercury to complete the circuit (inset picture of the fabricated Hg-MOSFET )

Therefore, the fabricated ISFET device was transformed into an Hg-MOSFET by depositing mercury on the sensing layer of the ISFET. A platinum reference electrode when in contact with the mercury provides required connection for the application of gate to source voltage as depicted in inset 5.5.f. The transfer and output characteristics of the Hg MOSFET are illustrated and explained in the result section.

### 5.4 Circuit diagram

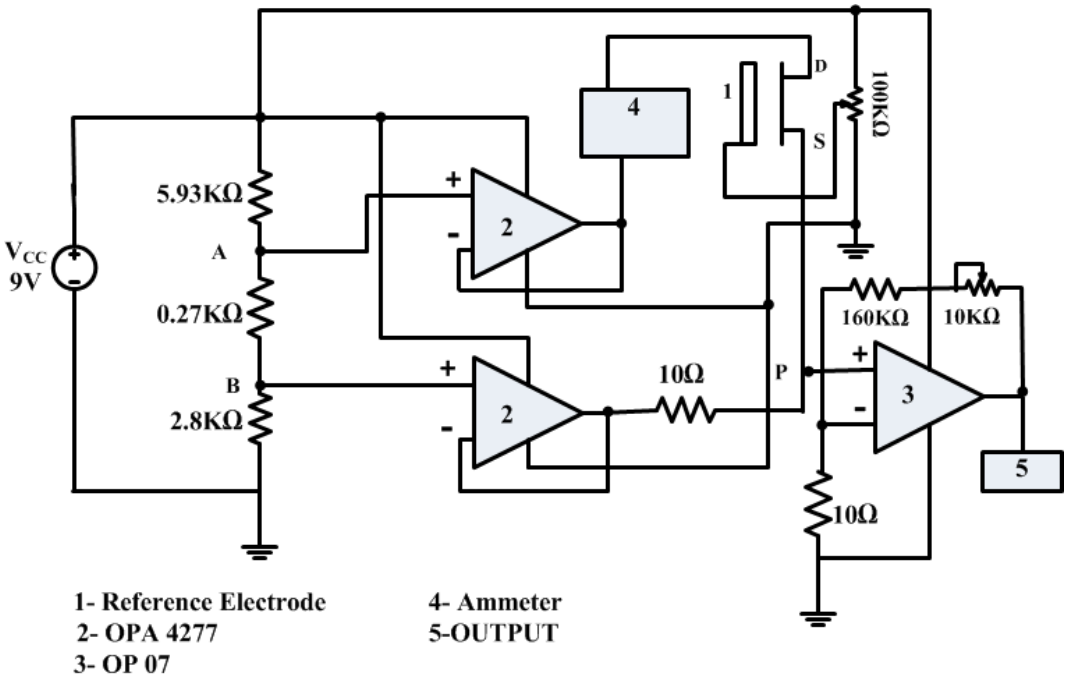


Figure.5.6. circuit diagram for the device characteristics

The schematic of the measurement set up for the ISFET and the CYPFET at constant applied potential difference is illustrated in the figure. 5.6. In this work, the characteristics of the devices are obtained using a constant voltage set up by keeping the potential difference between drain and source ($V_{DS}$) constant at 0.27V and varying the gate to source voltage ($V_{GS}$). Further, the corresponding drain current for different pH values is measured. Three resistances of value 5.93 kΩ, 0.27 kΩ and 2.8 kΩ were connected between $V_{cc}$ and A, A and B and between B and ground respectively. When 9V $V_{cc}$ is applied, the potential at point A and B with respect to the ground is 3.07 V and 2.8V respectively. The potential difference between the points A and B was set at desired value of 0.27V using this configuration. The circuit with OPA4277 high precision quad operational

amplifier (op-amp) was used as voltage follower to maintain the constant potential difference between the drain and source terminal. Since a voltage divider is used in the previous stage, op-amp has to be used as voltage follower so that adequate voltage will be supplied to the load. Therefore, OPA4277 has been chosen which has low input bias current (1 nA) and high input impedance (100 MΩ). The variable gate voltage of range 0-9V was applied using a multi-turn wire-wound potentiometer. The voltage output at point P had a low magnitude hence amplification was done. The amplification was achieved using a non-inverting JFET based op amp OP-07. This same circuit was also used to measure the device characteristics of CYPFET i.e., ISFET with immobilized bioreceptor CYP450.

The block diagram of the measurement set up for the output characteristics is depicted in the figure. 5.7. In the circuit described, the gate to source voltage can be varied using the potentiometer of value 10KΩ. Separate power was given to the gate terminal as the Keithley 6517B Electrometer is two terminal device. A stable potential difference was maintained at the reference electrode using a voltage follower (OP07). For the measurement, $V_{GS}$ was kept constant and $V_{DS}$ was varied from 0V to 9V using the Keithley Electrometer and the corresponding drain current were noted using the same electrometer as it is connected in series with the drain to source terminal.

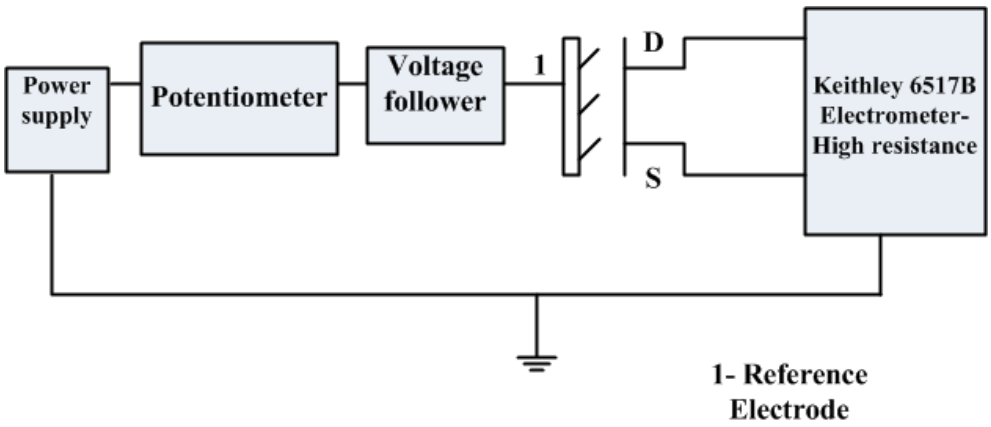


Figure 5.7. Block diagram for measurement set up for output characteristics

The actual set up with the fabricated device both for device characteristics measurement and output characteristics are depicted in the figure 5.8 a and b respectively.

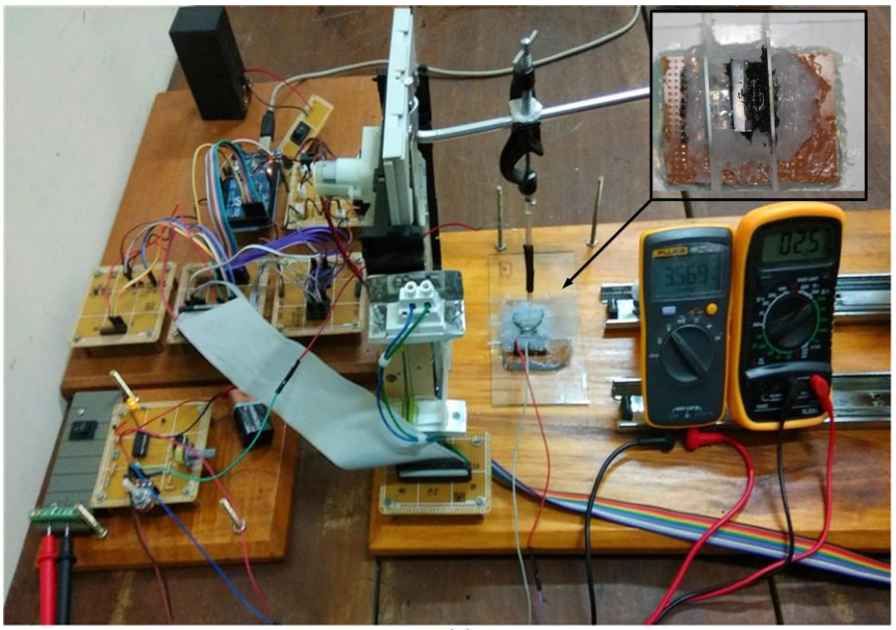

(a)

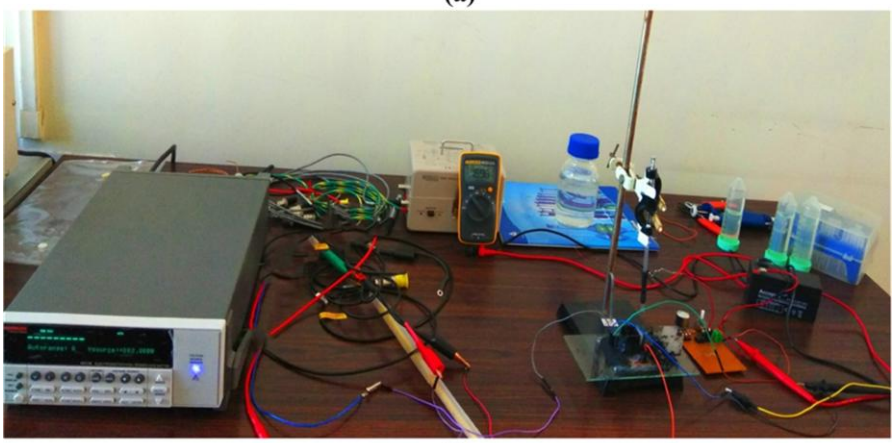

(b)

Figure. 5.8. (a) the actual measuring setup for device characteristics along with the fabricated device (inset: actual fabricated ISFET device), (b) Measuring setup of the output characteristics using Keithley 6517B electrometer.

### 5.5 Results and Discussion

Silicon dioxide was thermally deposited forming the sensing layer of the fabricated ISFET device. $SiO_2$ has lower sensitivity compared to many other materials but in this work, it was considered for the fabrication process because of its biocompatibility [26]. The potential developed at electrolyte/oxide interface is due to the interaction of the active sites of $SiO_2$ and the ions present in the electrolyte. Redistribution of charges results into the change in the surface charges which form the electrical double layer. This modifies the threshold voltage of the device. Any change in the pH of the solution is well detected from any change in the drain current. This change can be compensated by the adjustment of the reference electrode potential.

Further, immobilization of the fabricated ISFET device with the enzyme CYP450 oxidizes the analyte n-hexadecane to n-hexadecanol. In the reaction as stated in equation 5.4 two protons are consumed which influences the gate potential. The variation in the concentration of the substrate brings about change in the interfacial potential thus making it a functional ENFET device for sensing n-hexadecane. With the help of proton NMR (JEOL, ECS-400) the production of the n-hexadecanol was verified and using the software DELTA (Version-4.3.6) the data analysis was carried out. The presence of both n-hexadecane and n-hexadecanol in the reaction mixture was verified with the help of the NMR spectroscopy (figure 5.9)

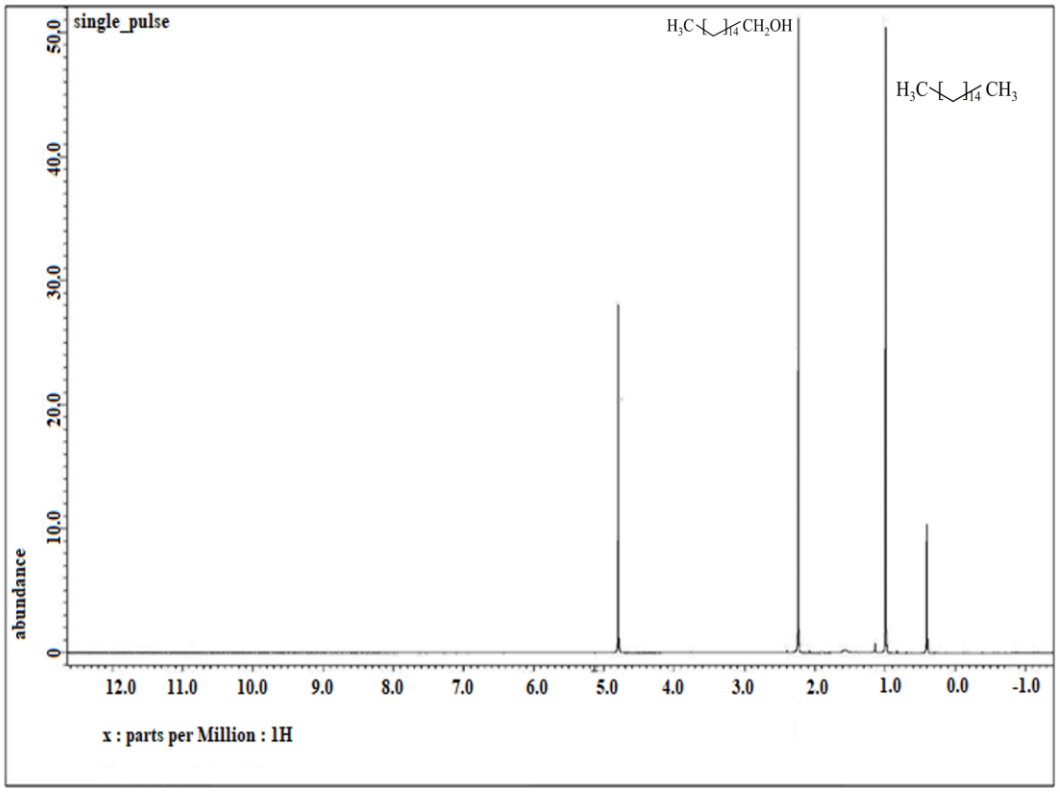


Figure.5.9 Proton NMR of the reaction mixture after the completion of the reaction

The reaction involved in the oxidation of the analyte is given as follows

$$H_{34}C_{16} + NADPH + O_2 \xrightarrow{CYP450} C_{16}H_{34}O + NADP^+ + H_2O \quad (5.4)$$

For the electrochemical measurements, platinum wire was used as the reference electrode instead of traditional Ag/AgCl electrode. The traditional electrodes have problems with the liquid junction. The silver (Ag) corrodes when not in use. Conversely, platinum wire can be used as pseudo-reference electrode for study of reaction kinetics. In addition, it has the advantage of being simple, convenient and with ease in operation [27].

The measurand used for ISFET measurement were Potassium Phosphate buffer (0.5 molar) for pH 6-10 and sodium citrate buffer (0.5 molar) for pH 4-5. For ENFET measurement, the solution used for analyte preparation was Potassium Phosphate buffer (0.05 molar, pH 7.2).

The device characteristics of the fabricated ISFET are illustrated in the following paragraphs. All the experiments were performed in triplicates with a significance value of less than 0.05.

### 5.5.1 Transfer Characteristics

The transfer characteristics relate the drain current of a device with that of the applied gate to source voltage. The gate current can be considered to be of zero value as the gate terminal is electrically isolated. The threshold voltage can be derived by extrapolating the curves obtained from $\sqrt{I_D}$ versus $V_{GS}$ plot [28]. Once the threshold voltage is attained the drain current increases as it indicates the onset of significant flow of drain current. In case of an ISFET device the threshold voltage is a function of pH value. The value increases with the decrease in the proton concentration. The threshold voltage of the fabricated ISFET device is found to be 1.95V, 2.05V and 2.2V for pH 4, 7 and 10 as depicted in figure 5.10 a, b and c respectively. Figure 5.10 d illustrates the transfer characteristics of the fabricated Hg-MOSFET device and is found to be 2.43V. Further, figure 5.10 e and f depict the transfer characteristics of the fabricated ENFET device. The enzyme which was immobilized was maintained at pH of 7.2. Hence the values are similar to pH 7. Therefore for 0.4M and 0.5M, it is found to be 2.08V and 2.095V respectively.

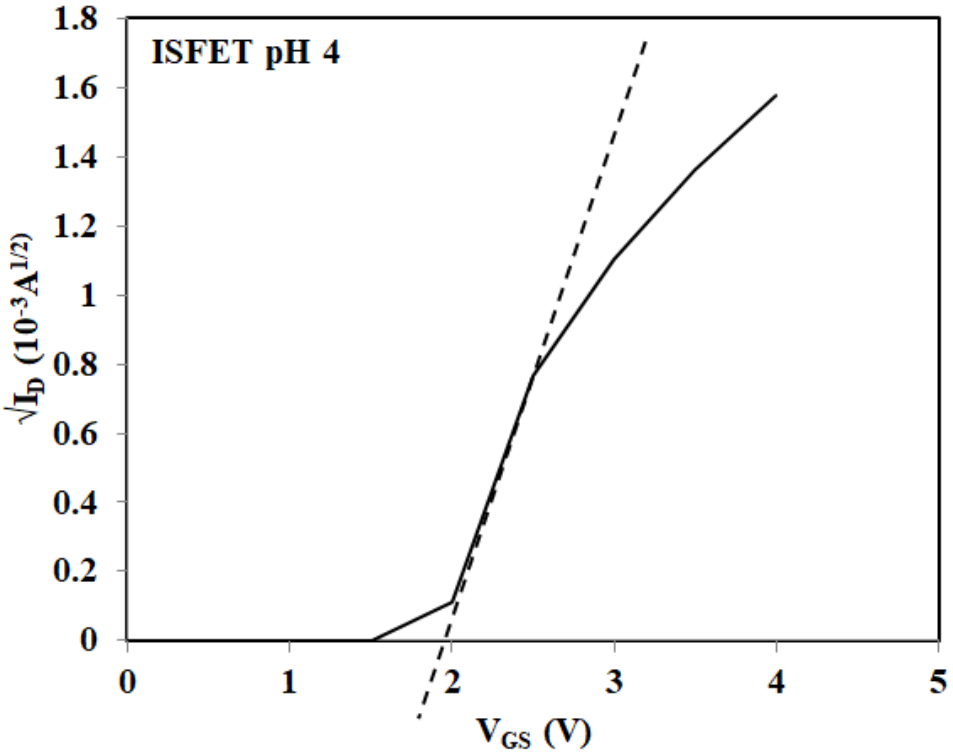


Figure 5.10 a. The $\sqrt{I_d}$ $vs$ $V_{GS}$ curve is plotted for pH 4

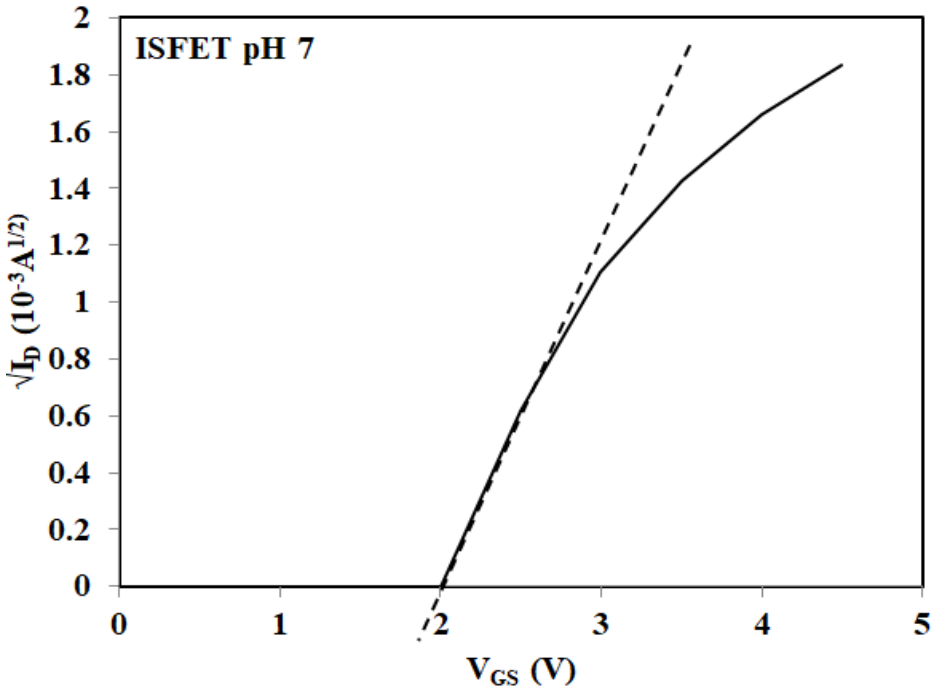


Figure 5.10 b. The $\sqrt{I_d}$ $vs$ $V_{GS}$ curve is plotted for pH 7

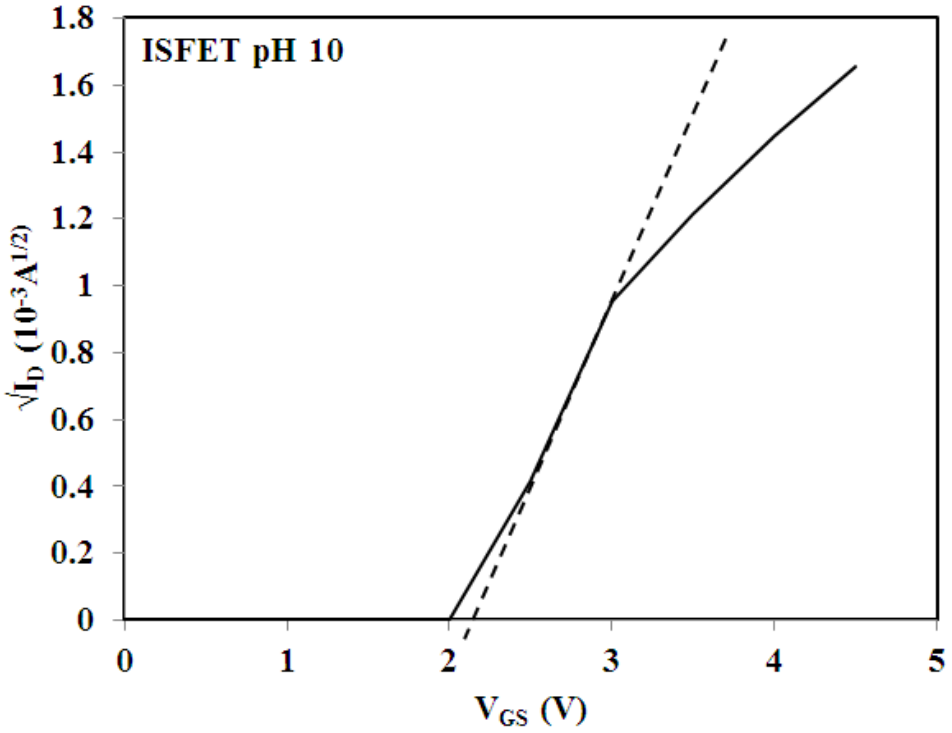


Figure 5.10 c. The $\sqrt{I_d}$ $vs$ $V_{GS}$ curve is plotted for pH 10

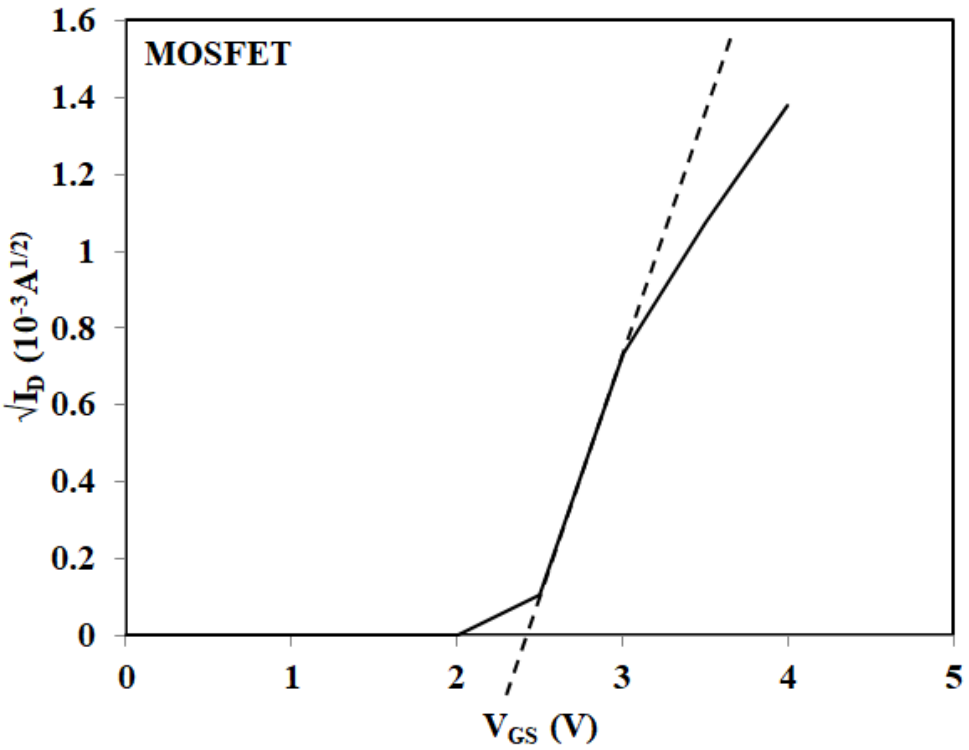


Figure 5.10 d. The $\sqrt{I_d}$ $vs$ $V_{GS}$ curve is plotted for MOSFET

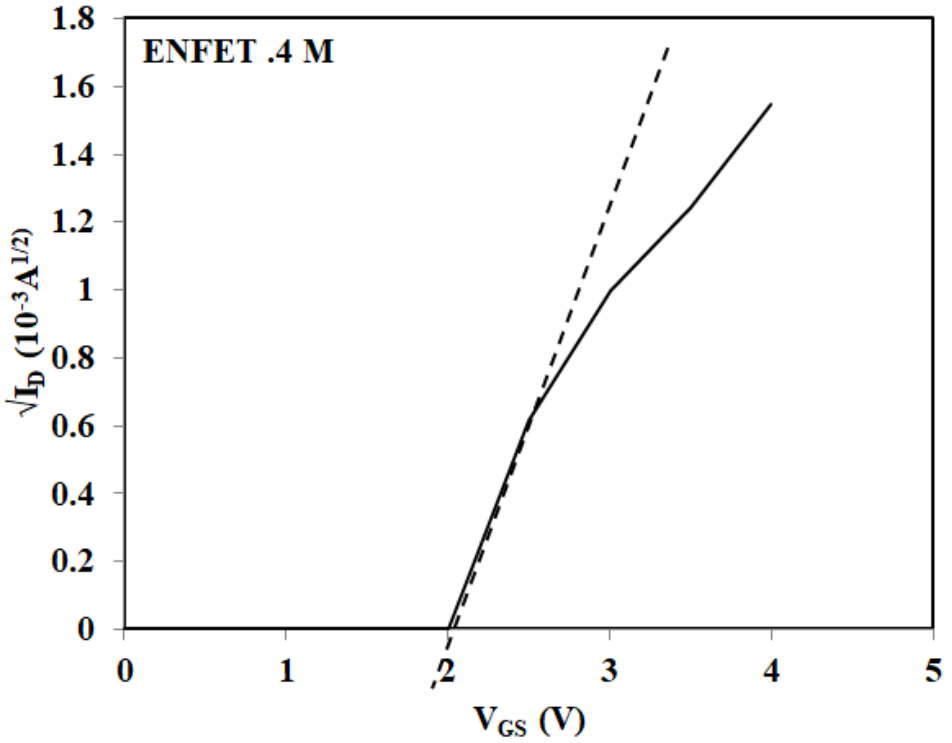


Figure 5.10 e. The $\sqrt{I_d}$ $vs$ $V_{GS}$ curve is plotted for 0.4 M ENFET

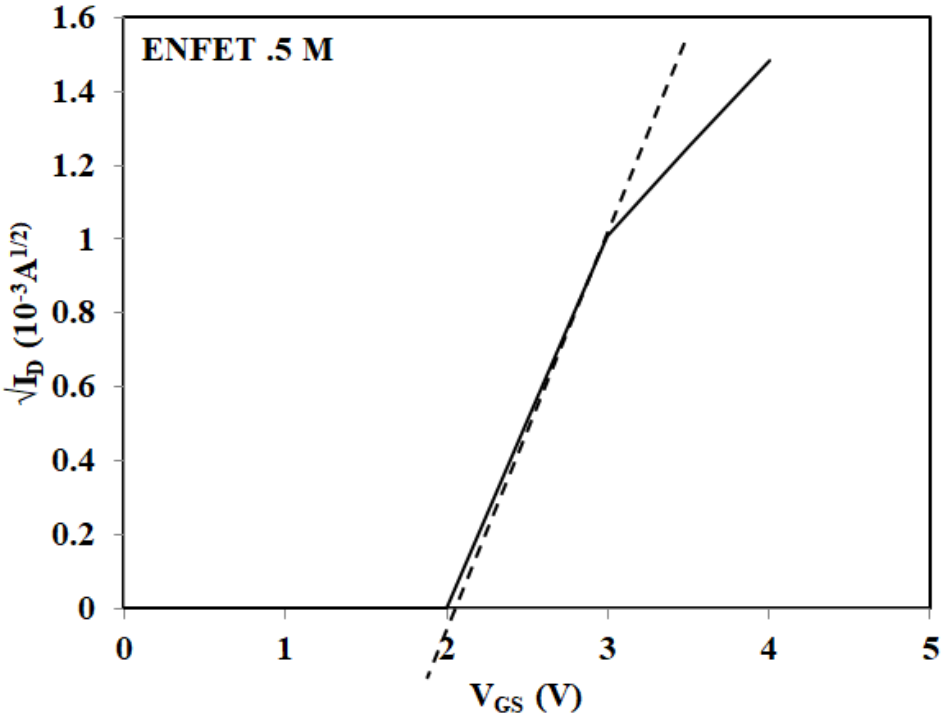


Figure 5.10 f. The $\sqrt{I_d}$ $vs$ $V_{GS}$ curve is plotted for 0.5 M ENFET

The drain current in an ISFET device depends on the potential drop at various interfaces as stated in the standard formula for calculation of threshold voltage (chapter 2 equation 2.2). However, most of the terms in the said equation are purely physical in nature. The interfacial electrolyte insulator potential termed as $\phi_{eo}$ which is present in the equation of the threshold voltage is mostly dependent on the pH of the electrolyte. Rest of the terms can be considered to be constant. Thus, the threshold voltage is defined as a function of pH [29] and the same is evident in figure 5.11. The threshold voltage obtained for the fabricated ISFET varies with the change in pH as indicated in the transfer characteristics section.

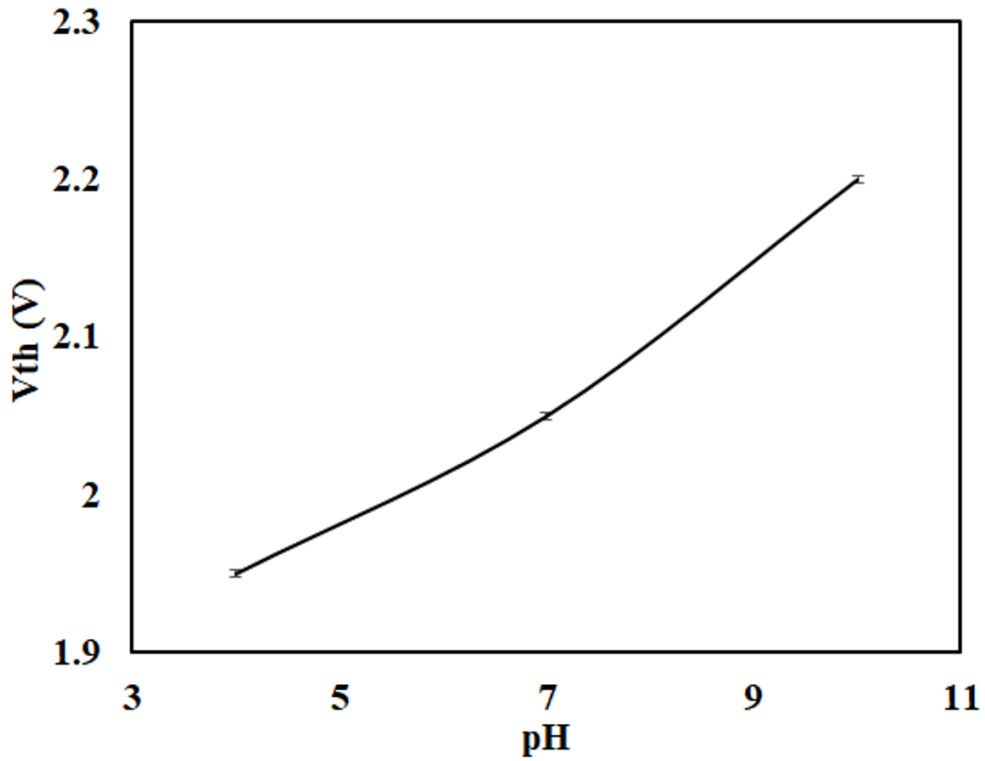


Figure 5.11. Variation of threshold voltage with respect to pH values of electrolyte

***Subthreshold swing***

The region before the device attains threshold voltage is the sub-threshold region of the operation. The subthreshold swing (SS) can be defined as the gate voltage required to change the drain current by one order of magnitude [30]. The $I_D$ was measured using the Keithley 6517B Electrometer. The $V_{GS}$ was varied from 1.9V to 2.5V and the log $I_D$ versus $V_{GS}$ was plotted. For the fabricated ISFET device, the SS is found to be 61mV/decade (for pH 7 at 27$^o$C) as illustrated in figure 5.12. The variation in gate voltage to achieve a decade change in drain current has been indicated by dotted lines intersecting the x axis before the threshold voltage. It is noteworthy that no change in SS has been observed with change in pH, which has also been reported in [31].

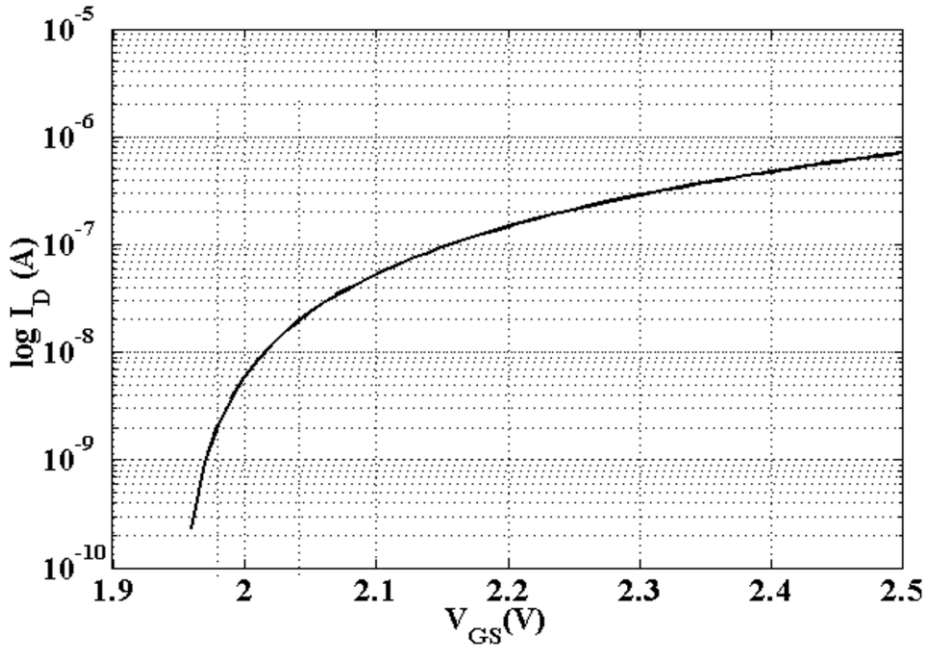


Figure 5.12. Subthreshold slope of the Schottky ISFET for pH 7

### 5.5.2 Output Characteristics

The output characteristics of the fabricated ISFET, Hg-MOSFET and ENFET are illustrated in figure 5.13. The gate to source voltage was kept constant at 3V and the drain to source potential varied from 0 to 5V. The drain current decreases with the increase in pH value. Further with mercury as gate over layer, the drain current decreases further. The buffer solution of the analyte is at pH 7.2. Hence the fabricated ENFET with two different molar concentrations of 0.4M and 0.5M shows similar trend as pH 7.

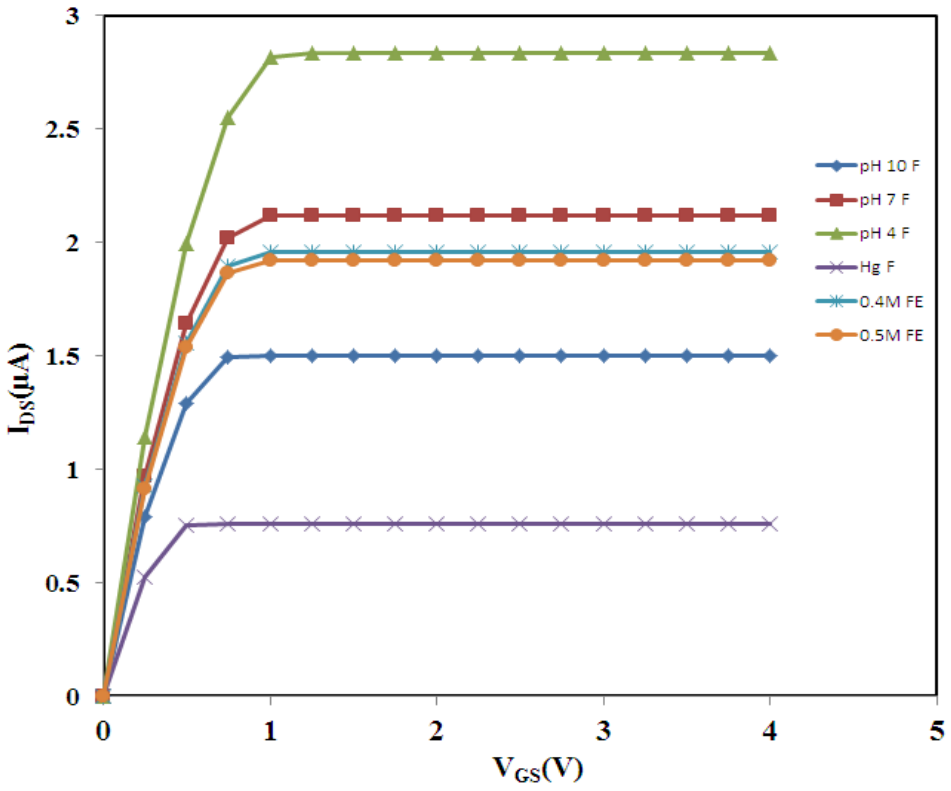


Figure 5.13. Output characteristics for the pH 4, pH 7 and pH 10 of fabricated ISFET , Hg MOSFET and 0.4molar and 0.5 molar ENFET is plotted. F indicates fabricated, FE indicates fabricated ENFET, Hg F indicates fabricated Hg MOSFET.

### 5.5.3 Sensitivity

The sensitivity of the fabricated ISFET device is described in terms of variation in $V_{GS}$ with respect to change in pH of the electrolyte. The sensitivity of the ENFET device is measured in terms of variation in the concentration of the analyte (here n-hexadecane). The parameter $V_{GS}$ required to maintain a constant current for different value of pH (pH 4 to 10) is measured to obtain the sensitivity ($S_{ISFET}$) of the device. Mathematically, the sensitivity of the ISFET device is expressed as

$$S_{ISFET} = \left.\frac{\Delta V_{GS}}{\Delta pH}\right|_{I_{DS}=Constant}$$

Variation in the applied $V_{GS}$ to maintain a constant current for pH ranging from acidic pH 4 to alkaline pH 10 is illustrated in figure. 5.14. The sensitivity of the device is measured for four different constant currents of 0-1.5 µA (step of 0.5 µA). It is evident from the figure that with the increase in pH value the $V_{GS}$ required to maintain a constant current is higher. The average sensitivity of the Schottky based ISFET calculated from the measured values is found to be about 50.65mV/pH.

Furthermore, three devices were fabricated in a batch with same dimension and fabrication procedure. The device with higher accuracy in sensitivity amongst these three devices was opted for development of ENFET. Figure 5.15 shows the sensitivities of the three ISFET devices (over a range of pH 4 to 10 at constant current of 0.5µA) and mean sensitivity for each device is found to be 50.65±2.38, 49.87±3.60 and 50.1±3.81mV/pH. Device 1 exhibited better sensitivity with the least deviation, therefore it was immobilized further to form ENFET.

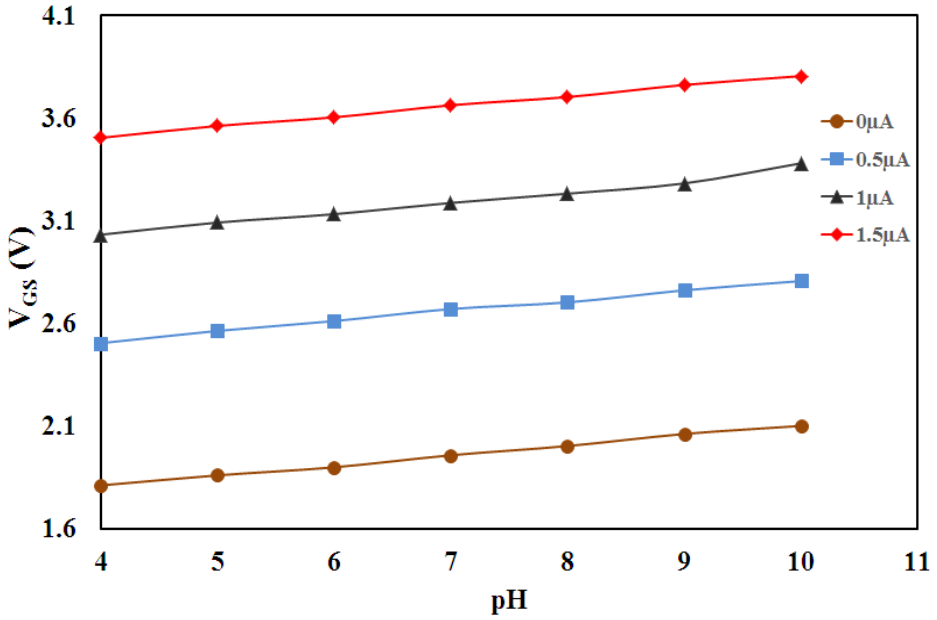


Figure. 5.14. Variation of $V_{GS}$ with respect to change in pH keeping current constant at 0, 0.5, 1.0 and 1.5μA respectively

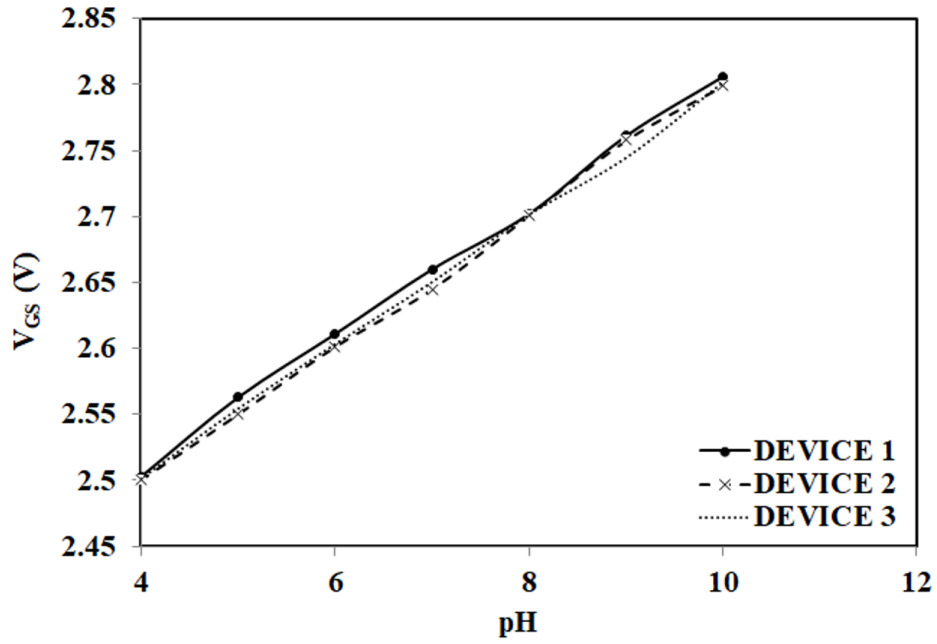


Figure 5.15. Variation in $V_{GS}$ value with respect to change in pH for constant current 0.5μA for the three devices fabricated in a batch

After the immobilization is done the variation in the gate to source potential is measured with the change in concentration of the analyte ($C$) at constant currents. Mathematically, the sensitivity of the ENFET is given as

$$S_{ENFET} = \left.\frac{\Delta V_{GS}}{\Delta C}\right|_{I_{DS}=Constant}$$

Figure 5.16 illustrates the variation in the $V_{GS}$ value with respect to the change in the concentration of the analyte (n hexadecane) which is made to vary from the range of 0.1 to 0.5mol/l (step of 0.1 mol/l) keeping the current constant at 0.5 and 0.75µA. The figure indicates that with the increase in the hydroxide ions in the solution due to the conversion of the analyte into the product (n-hexadecanol), the value of $V_{GS}$ increases. The sensitivity obtained from the curve indicates that the fabricated ENFET is about 54.34mV/molar.

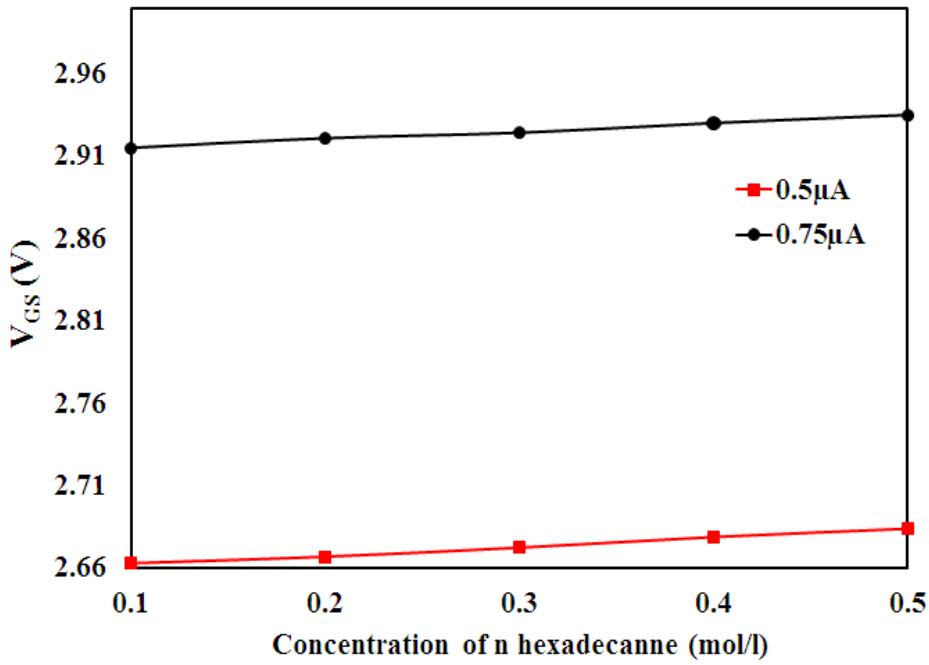


Figure.5.16. Variation of $V_{GS}$ with respect to change in concentration of n hexadecane at constant currents 0.5 µA and 0.75µA respectively.

### 5.5.4 Stability

After the device has been immobilized to form ENFET, results were monitored continuously for three consecutive days with a period gap of 24 hours. The device during the monitoring period was kept at room temperature (27$^{o}$C) and without the Potassium Phosphate buffer solution. During the measurement period, variation in $V_{GS}$ is measured with the change in concentration of n hexadecane for two constant currents of 0.5 and 0.75 µA as depicted in figure 5.17 a and b respectively. Repeatability test conducted for day 1 and day 2 showed that the variation in the results between the days is reasonably low. This infact indicates that the fabricated device has the potential to be used as a biosensor for hydrocarbon detection. However, the results start to decline from the third day onwards.

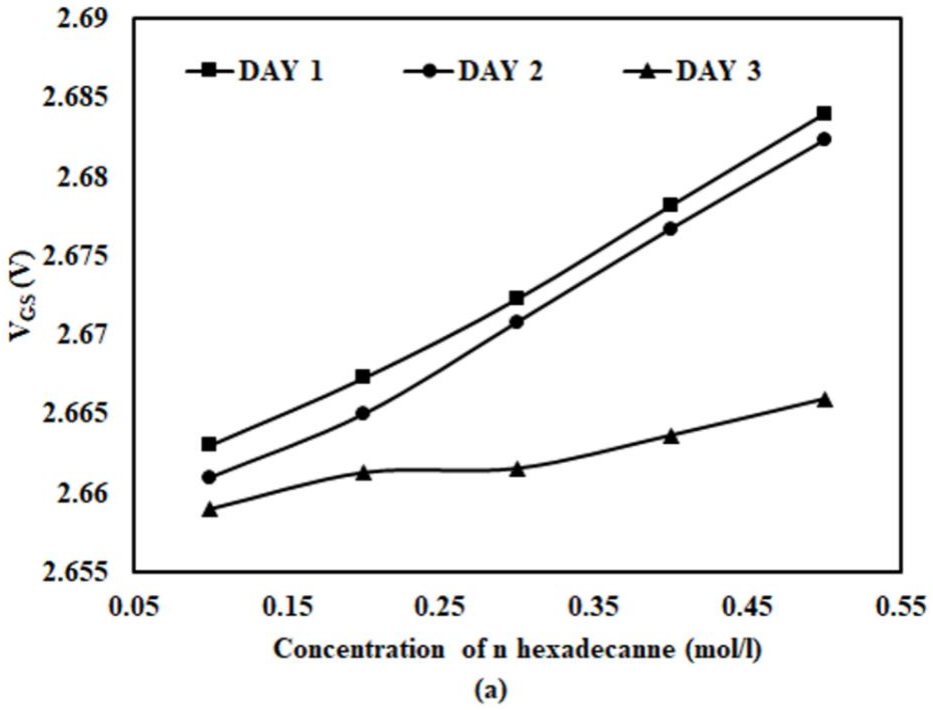


Figure 5.17a Variation of $V_{GS}$ with respect to concentration of n hexadecane measured at three consecutive days for constant current of 0.5 µA

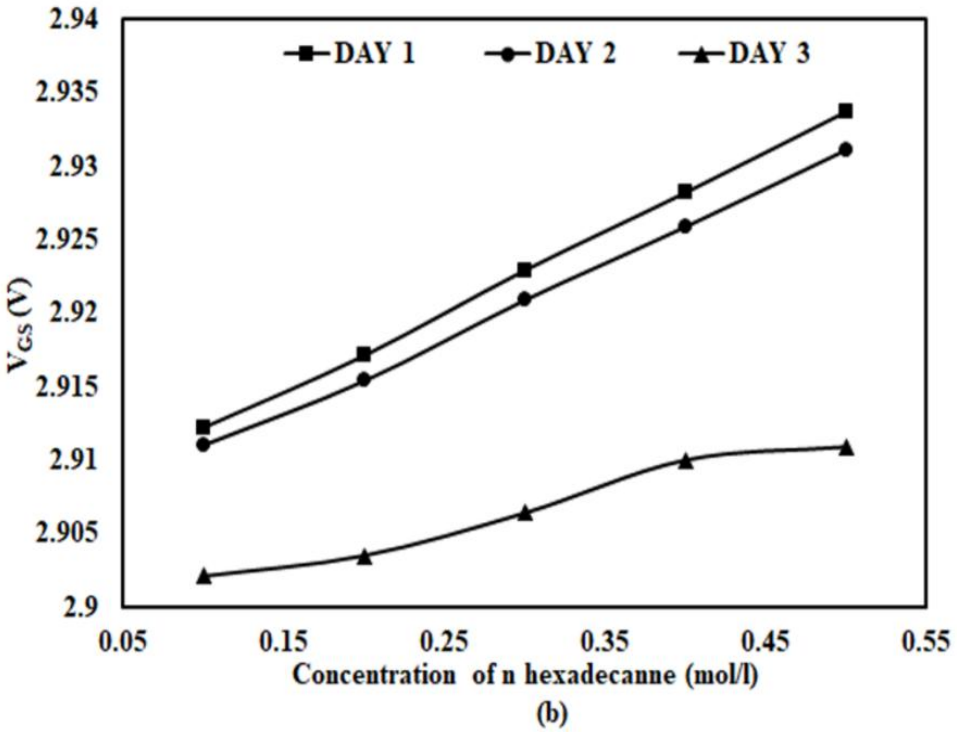


Figure 5.17 b. Variation of $V_{GS}$ with respect to concentration of n hexadecane measured at three consecutive days for constant current of 0.75μA

### 5.5.5 Hysteresis

Hysteresis is a characteristic of the sensor device which indicates its instability. Hysteresis observed in $SiO_2$ ISFET in literature has been related to ion in-diffusion [32] and buried OH sites [33]. The formation condition impacts the relationship of the pH sensitivity with that of the concentration of OH groups in the oxide as stated in a published report [34]. Hysteresis is measured as the difference in sensor output signal between the upward and downward series of a measurement cycle. In figure 5.18(a) the forward and backward path along with the hysteresis observed in the fabricated Schottky based ISFET is illustrated. Here upward path followed (for $I_{DS}$ =0.5 μA from pH 4 to 10) is A →B→C and downward path (from pH 10 to 4) is C→D→E. Similarly the hysteresis path for current of 0.75 μA is as P→Q→R→S→T. The average error in sensitivity of fabricated Schottky based ISFET caused by hysteresis was found to be around ±0.3-0.4%. Further for the cytochrome based ENFET, the hysteresis path is shown in fig 5.18(b) as A→B→C→D→A. The average error in sensitivity for the ENFET caused by hysteresis was found to be around ±0.015%.

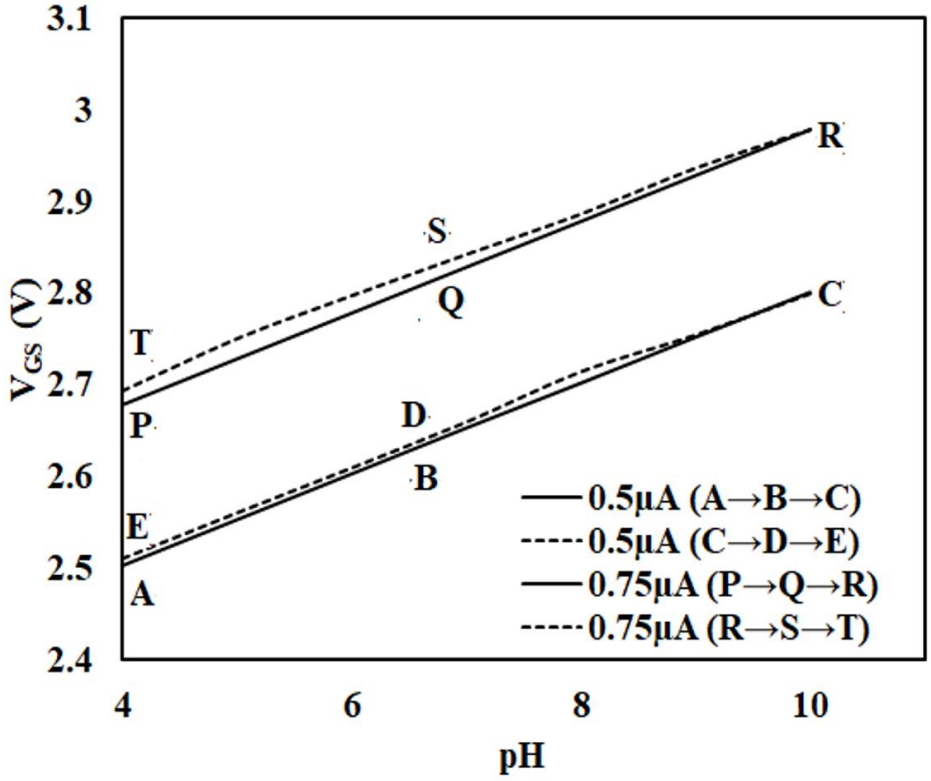


Figure. 5.18 a. Hysteresis observed in the fabricated ISFET device

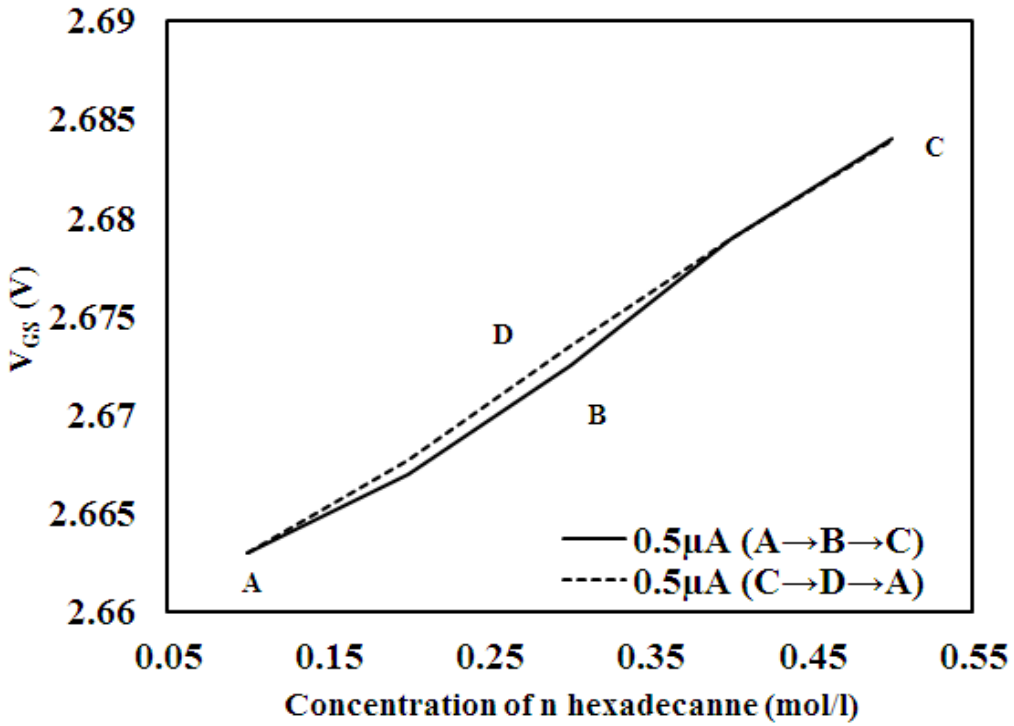


Figure. 5.18 b. Hysteresis observed in the fabricated ENFET device

### 5.5.6 Detection limit and change in pH after reaction

The samples after the enzymatic reaction has been carried out are collected and the pH is measured. This was done to examine the variation in pH value with the change in the concentration of the analyte. Standard pH meter was used to observe the change in pH. In the figure 5.19, it indicates that there is almost a linear increase in pH value with the change in concentration from 0.1 to 0.5mol/l. A negligible change was observed when the concentration was considered for 0.001 to 0.0001 mol/l (Figure. 5.19 inset). Thus the limit of the sensor is found to be about 0.01mol/l.

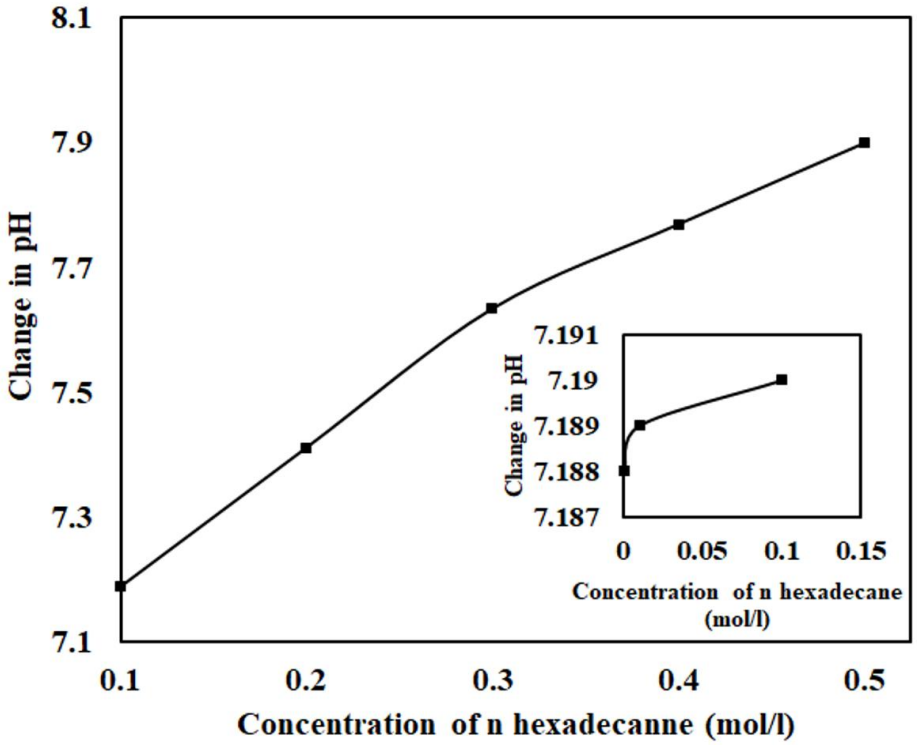


Figure. 5.19. Change in pH with respect to concentration of the n-hexadecane

### 5.5.7 Reproducibility of the sensor system

The reproducibility of the sensor system was observed by considering the measurement by the sensor of the emulsions of different concentration of the analyte in a 50mM of Tris HCl buffer kept at a pH of 7.2. For three consecutive days, the experiment was conducted for every 12 hours. Figure 5.20 illustrates the reproducibility of the sensor system considered for a particular current 0.5µA, and it was observed that it could be reproduced well up to four cycles (48 hours). Degradation was observed after the end of four cycles. This may be due to deterioration of the enzyme protein.

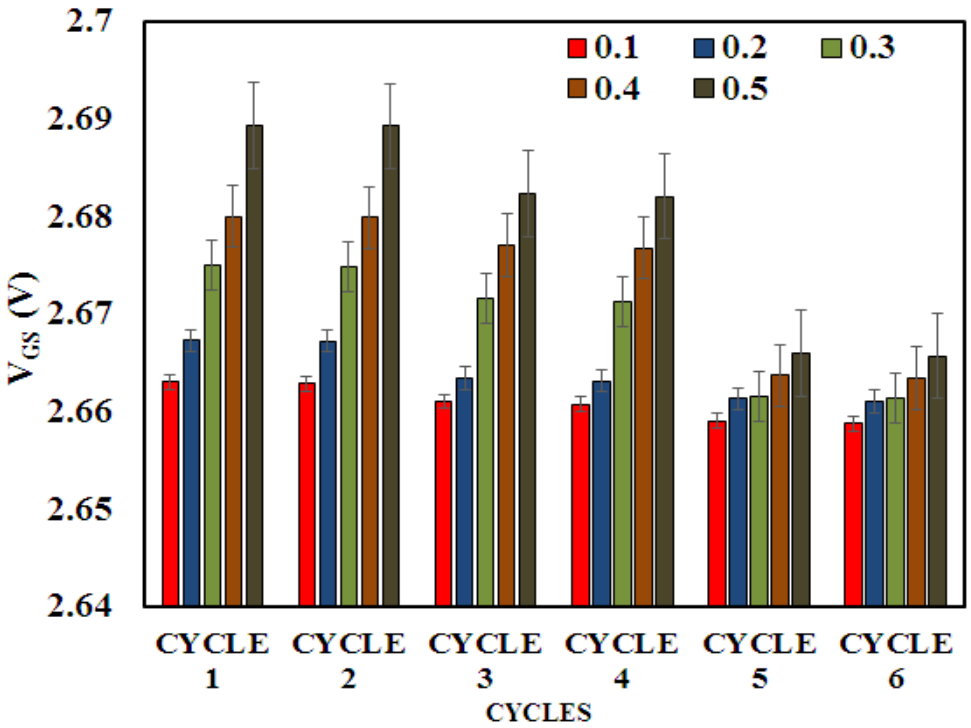


Figure 5.20. Reproducibility of sensor output for a particular current 0.5µA for 6 cycles (72 hours; 12 hours each) for 0.1 to 0.5 mol/l

### 5.5.8 Procedure for measurement of n hexadecane

When the concentration of n hexadecane is unknown, it can be obtained from the regression equation. Say for example when a particular current 0.5µA is being considered the unknown analyte concentration (n-hexadecane) can be obtained from the standard curve as indicated in figure 5.21. The correlation coefficient is found to be 0.9848 and the regression equation is obtained as

$$y = 0.0653x + 2.6553$$

(X-values assays the concentration of analyte (n-hexadecane) depending on the Y-values).

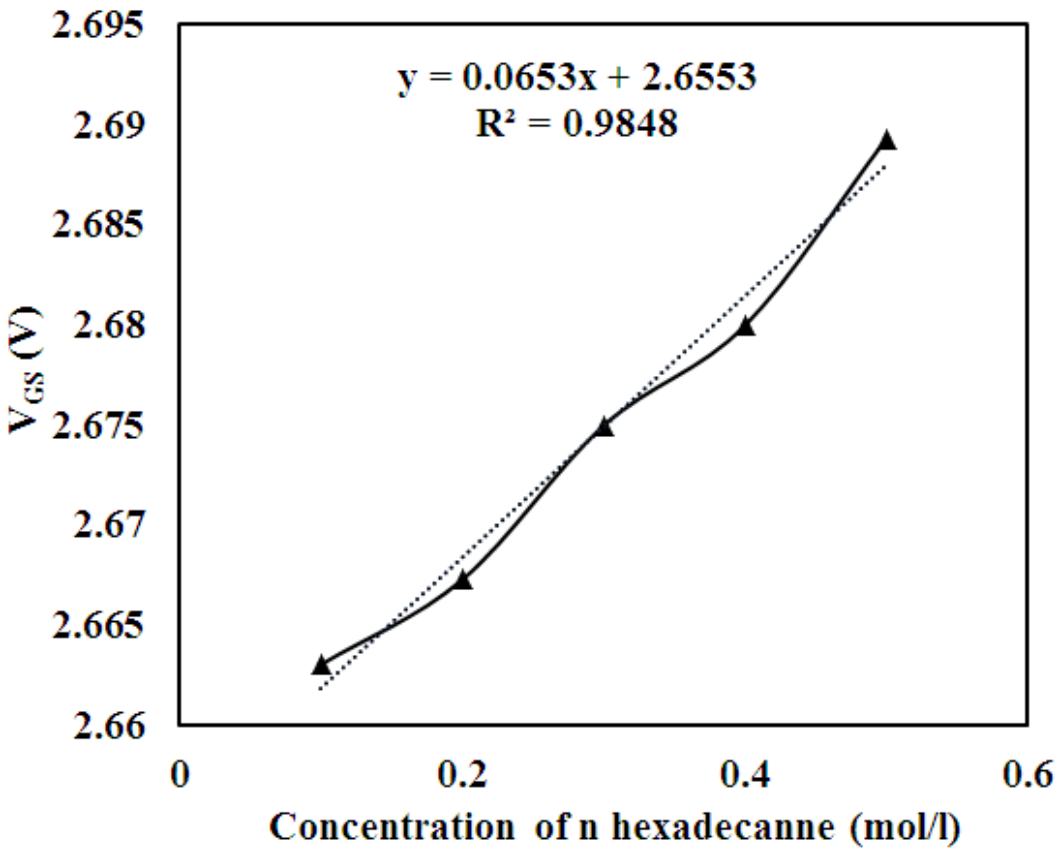


Figure. 5.21. Correlation and regression line for measurement of n hexadecane assayed by the fabricated sensor.

### 5.5.9 Convertibility of the fabricated ISFET

As indicated earlier in this chapter the fabricated ISFET is made into a ENFET and also into a Hg-MOSFET. The fabrication process involved in this work is simple, cost effective and involves minimal number of steps. The fabricated ISFET is converted into Hg-MOSFET and tested. Then after the removal of Hg the same device is immobilized to form ENFET. This enzyme is removed easily with the use of luke warm water and the original ISFET device is retrieved back. This process of conversion was continued for a period of 100 days with multiple transformations from one form to another. It was observed that there is no visible degradation in the sensitivity of the fabricated original ISFET device. Figure 5.22 indicates this as the variation of $V_{GS}$ was measured for pH 4, 7 and 10 at constant current(0.5 µA) was observed after it was made into Hg – MOSFET and Cytochrome P450 ENFET and the original device retrieved back. The conversion was done from one form to another for every 72 hours and the ISFET sensitivity was measured after an interval of 20 days for a period of 100 days. To maintain the above mentioned current, the $V_{GS}$ was measured and found to be 2.50V±0.25mV, 2.67V±0.4mV, and 2.81V±0.6 mV for pH 4, 7 and 10 respectively proving high stability of the device even after repeated conversions from one form to another.

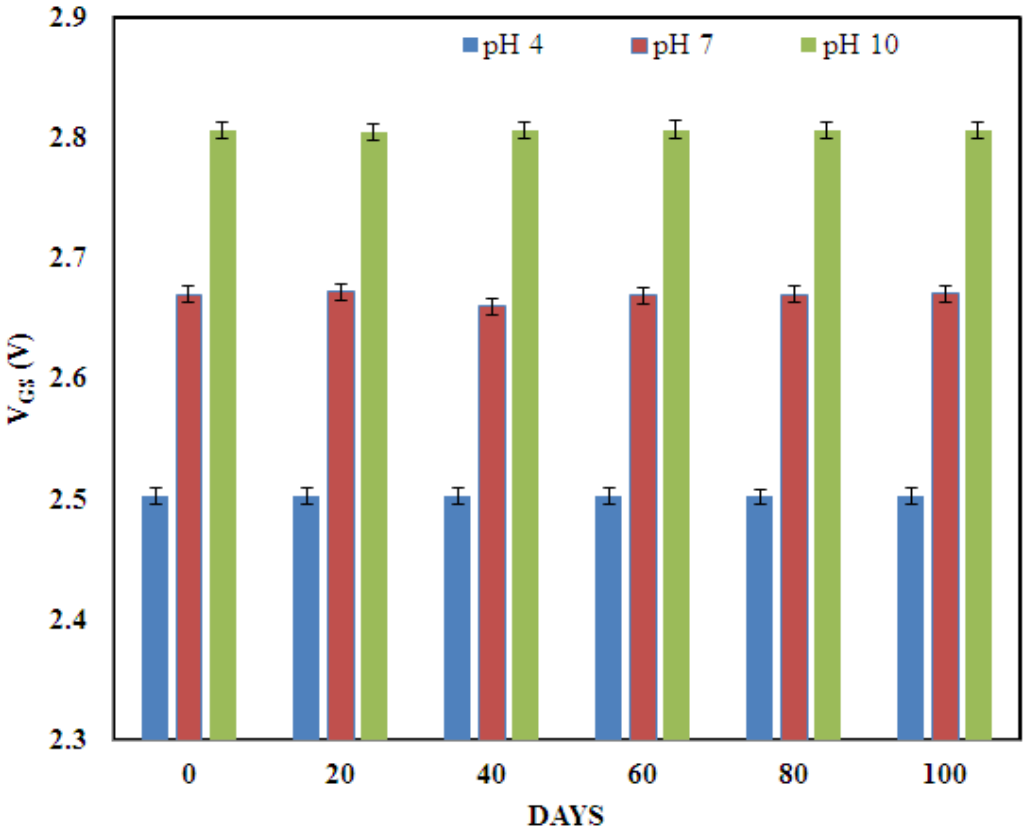


Figure. 5.22. Variation of $V_{GS}$ for the fabricated ISFET device at current 0.5µA for pH 4, 7 and 10 with the repeated conversions from ISFET to MOSFET/ENFET and vice versa in a time period of 100 days.

### 5.5.10 Comparative analysis

The present machines involved in hydrocarbon detection are bulky and costly, therefore a portable and cost effective sensor would be more efficient and convenient for monitoring pollution caused by hydrocarbons. Researchers have developed several sensors capable of detecting hydrocarbons, involving different techniques from simple electrode based sensors to fibre optics [35,36]. Table 5.1 illustrates a comparison of different techniques and detection limit of various sensors for hydrocarbon detection.

TABLE 5.1

COMPARISON OF VARIOUS SENSORS USED FOR HYDROCARBON DETECTION

| **Sensor Type** | **Technique** | **Analyte for detection (Hydrocarbon)** | **Detection limit** | **Reference** |
|---|---|---|---|---|
| Optical | Optical-Fiber Sensor | Alkane (Small alkane in vapour form) | | [37] |
| Electronic noses (Gas Sensor) | Metal Oxide Semiconductor (MOS) Sensor using SOMMSA approach | Alkanes, alcohols, aldehydes, ketones, acids and esters (small molecules up to C10 in vapour form) | 0.48 µmol/ml | [38] |
| Chemical Sensor | Colorimetric sensor | Aliphatic Hydrocarbons (C5-C14) | | [39] |
| Gas sensor | Thermoelectric Hydrocarbon Sensors | Alkane (Small alkane in vapour form) | 162 µmol/ml | [35] |
| Electrochemical Biosensor | ENFET | Alkane (C16) | 0.01 mol/l | Our device |

**Bibliography**

[1] Nishi, Y. Insulated gate field effect transistor and its manufacturing method. Japan Patent. 587(527):162-165, Apr. 1970.

[2] Lepselter, M.P. and Sze, S.M. SB-IGFET: An insulated-gate field-effect transistor using Schottky barrier contacts for source and drain. *Proceedings of the IEEE*, 56(8):1400-1402, 1968.

[3] Mochizuki, T. and Wise, K.D. An n-channel MOSFET with Schottky source and drain. *IEEE electron device letters*, 5(4):108-111, 1984.

[4] Oh, C.S., Koh, Y.H., and Kim, C.K. A new P-Channel MOSFET structure with Schottky-Clamped source and drain. In *Electron Devices Meeting, 1984 International*, pages 609-612, 1984.

[5] Tsui, B.Y. and Chen, M.C. A Novel Process for High-Performance Schottky Barrier PMOS. *Journal of The Electrochemical Society*, 136(5):1456-1459, 1989.

[6] Sugino, M., Akers, L.A., and Rebeschini, M.E. CMOS latch-up elimination using Schottky barrier PMOS. In *Electron Devices Meeting, 1982 International*, pages 462-465, 1982.

[7] Swirhun, S.E., Sangiorgi, E.N., Weeks, A.J., Swanson, R.M., Saraswat, K.C., and Dutton, R.W. A VLSI-suitable Schottky-barrier CMOS process. *IEEE Journal of Solid-State Circuits*, 20(1):114-122, 1985.

[8] Tucker, J.R., Wang, C., and Carney, P.S. Silicon field-effect transistor based on quantum tunneling. *Applied Physics Letters*, 65(5):618-620, 1994.

[9] Snyder, J.P. *The physics and technology of platinum silicide source and drain field-effect transistors*. PhD thesis, Stanford University, 1997.

[10] Grattarola, M. and Massobrio, G. *Bioelectronics handbook*. McGraw-Hill, 1998.

[11] Muller, R.S., Kamins, T.I., Chan, M., and Ko, P.K. *Device electronics for integrated circuits*. Wiley, New York, 2003.

[12] Larson, J.M. and Snyder, J.P. Overview and status of metal S/D Schottky-barrier MOSFET technology. *IEEE Transactions on Electron Devices*, 53(5):1048-1058, 2006

[13] Calvet, L.E. *Electrical Transport in Schottky Barrier MOSFETs*, PhD thesis, Department of Electronics and Communication Engineering , Yale University, 2001.

[14] Vega, R.A. Schottky field effect transistors and Schottky CMOS circuitry. Master's thesis, Department of Microelectronics Engineering, Rochester Institute Technology, Rochester, New York, 2006.

[15] Shimada, T. and Kuriyama, Y. F. Metabolic activation of polycyclic aromatic hydrocarbons to carcinogens by cytochromes P450 1A1 and1B1, *Cancer science*, 95:1-6, 2004.

[16] Ortiz De Montellano, P.R. and De Voss, J.J. Substrate oxidation by cytochrome P450 enzymes. In *Cytochrome P450: Structure, Mechanism and Biochemistry*, pages 183-245.Kluwer Academic/Plenum Publishers Springer, New York, 2005.

[17] Furge, L.L and Guengerich, F.P. Cytochrome P450 enzymes in drug metabolism and chemical toxicology: An introduction. *Biochemistry and Molecular Biology Education*, 34(2):66-74, 2006.

[18] Ortiz de Montellano, P.R. Hydrocarbon hydroxylation by cytochrome P450 enzymes, *Chemical reviews*, 110:932-948, 2009.

[19] Omura, T. and Sato, R. The carbon monoxide-binding pigment of liver microsomes I. Evidence for its hemoprotein nature, *Journal of Biological Chemistry*, 239:2370-2378, 1964.

[20] Phillips, I.R. , Shephard, E., and Ortiz de Montellano, P.R. *Cytochrome P450 Protocols*, Humana Press Inc, Totowa, 2013.

[21] Agrawal, V. and Miller, W.L. P450 oxidoreductase: Genotyping, expression, purification of recombinant protein, and activity assessments of wild-type and mutant protein, *Cytochrome P450 Protocols*, pages 225-237, 2013.

[22] Hara, M., Yasuda, Y., Toyotama, H., Ohkawa, H., Nozawa, T., and Miyake, J. A novel ISFET-type biosensor based on P450 monooxygenases, *Biosensors and Bioelectronics*, 17:173-179, 2002.

[23] Modi, B. P., Mathai, A. J., Patel, K. D., Pathak, V. M., and Srivastava, R. Stability of liquid metal Schottky contacts. *Indian Journal of Pure & Applied Physics*, 43(3):184-187, 2005.

[24] Werner, J. H., and Güttler, H. H. Barrier inhomogeneities at Schottky contacts. *Journal of applied physics*, 69(3):1522-1533, 1991.

[25] Kraack, H., Ocko, B.M., Pershan, P.S., Sloutskin, E., and Deutsch, M. Langmuir films of normal-alkanes on the surface of liquid mercury. *The Journal of chemical physics*, 119(19):10339-10349, 2003.

[26] Voskerician, G., Shive, M.S., Shawgo, R.S., Von Recum, H., Anderson, J.M., Cima, M.J., and Langer, R. Biocompatibility and biofouling of MEMS drug delivery devices, *Biomaterials*, 24:1959-1967, 2003.

[27] Kasem, B.K.K. and Jones, S. Platinum as a reference electrode in electrochemical measurements, *Platinum Metals Review*, 52:100-106, 2008.

[28] Ortiz-Conde, A., Sánchez, F.G., Liou, J.J., Cerdeira, A., Estrada, M., and Yue, Y. A review of recent MOSFET threshold voltage extraction methods. *Microelectronics Reliability*, 42(4-5):583-596, 2002.

[29] Bergveld, P. Thirty years of ISFETOLOGY: What happened in the past 30 years and what may happen in the next 30 years, *Sensors and Actuators B: Chemical*, 88:1-20, 2003.

[30] J. P. Uyemera, *CMOS logic circuit design*, Springer Science & Business Media, 1999.

[31] Back, J.H. and Shim, M. pH-dependent electron-transport properties of carbon nanotubes. *The Journal of Physical Chemistry B*, 110(47):23736-23741, 2006.

[32] Zemel, J.N. Microfabricated nonoptical chemical sensors, *Review of scientific instruments*, 61:1579-1606, 1990.

[33] Bousse, L. and Bergveld, P. The role of buried OH sites in the response mechanism of inorganic-gate pH-sensitive ISFETs, *Sensors and Actuators*, 6:65-78, 1984.

[34] Vlasov, Y., Tarantov, Y., Letavin, V., and Baraban, A. physicochemical processes occurring in ion-selective field-effect transistors (ISFT)-sensitivity to fluoride ions of electrolyte solution-$SiO_2$-Si systems used in ion-selective field-effect transistors, *Journal of applied Chemistry of the ussr*, 55:1201-1204, 1982.

[35] Kita, J., Hagen, G., Schmitt, C., and Moos, R. Sensitivity Improvement of Thermoelectric Hydrocarbon Sensors: Combination of Glass-Ceramic Tapes and Alumina Substrates. In *Multidisciplinary Digital Publishing Institute Proceedings*, volume 1, pages 403-406, 2017.

[36] Wollenberger, U., Neumann, B., and Scheller, F.W. Development of a biomimetic alkane sensor. *Electrochimica acta*, 43(23):3581-3585, 1998.

[37] Ronot, C., Gagnaire, H., Goure, J. P., Jaffrezic-Renault, N., and Pichery, T. Optimization and performance of a specifically coated intrinsic optical-fibre sensor for the detection of alkane compounds. *Sensors and Actuators A: Physical*, 42(1-3):529-534, 1994.

[38] Kohl, D., Heinert, L., Bock, J., Hofmann, T., and Schieberle, P. Systematic studies on responses of metal-oxide sensor surfaces to straight chain alkanes, alcohols, aldehydes, ketones, acids and esters using the SOMMSA approach. *Sensors and Actuators B: Chemical*, 70(1-3):43-50, 2000.

[39] Park, D. H., Hong, J., Park, I. S., Lee, C. W., and Kim, J. M. A Colorimetric Hydrocarbon Sensor Employing a Swelling Induced Mechanochromic Polydiacetylene. *Advanced Functional Materials*, 24(33),5186-5193, 2014.